

## Crystallization studies of doped SbTe phase-change thin films and PRAM line cells: Growth rate determination by automated TEM image analysis

Jasper Oosthoek<sup>a</sup>, Bart J. Kooi<sup>a\*</sup>, Jeff De Hosson<sup>a</sup>,  
Dirk Gravesteijn<sup>b</sup>, Karen Attenborough<sup>b</sup>, Rob Wolters<sup>c</sup>, Marcel Verheijen<sup>d</sup>

- Zernike Institute for Advanced Materials and Materials Innovation Institute M2i, University of Groningen, Nijenborgh 4, 9747 AG, Groningen, The Netherlands.
- NXP-TSMC Research Center, Kapeldreef 75, 3001 Leuven, Belgium
- NXP-TSMC Research Center, High Tech Campus 4, 5656 AE Eindhoven, The Netherlands
- Philips Research, High Tech Campus 4, 5656 AE Eindhoven, The Netherlands

### ABSTRACT

Crystal-growth rates in amorphous fast growth phase-change layers and a FIB processed phase-change random access memory (PRAM) line cell were measured at various temperatures using *in situ heating* in a transmission electron microscope. A procedure is presented here that allows the computer controlled detection of the position of the amorphous-crystalline interface in an image and subsequently, from a time series of images the computer controlled quantification of the pure crystal growth rate is determined. The growth rate (without nucleation) of the fast-growth material in the blanket layers is of interest for comparison with the identical material used in the PRAM line cells.

The activation energy for growth in the blanket films as measured by *in situ* TEM was found to be 3.0 eV. The activation energy related to the retention times of the PRAM line cells as measured by *in situ* heating and electrical characterization in a probe station was found to be 2.7 eV. More interestingly the equivalent retention times calculated for the blanket layers are much higher than the retention times observed for the PRAM line cells; a shift of about 25 °C occurs.

The procedures developed and presented here for detecting interfaces and for quantifying growth rates can be useful for a wide range of applications.

**Key words:** PRAM, line cell, TEM, blanket layer.

### 1. INTRODUCTION

A quantitative analysis of crystal growth in a series of images is of importance for the field of phase-change materials.<sup>1</sup> Crystal growth in amorphous films is the rate-limiting step in rewritable data storage. These materials have been successfully applied in rewritable optical recording based on the well-known CD, DVD<sup>2</sup> and Blu-Ray Disk<sup>3</sup> formats. Currently, phase-change materials are extensively tested as the storage element in nonvolatile solid-state electrical memory generally called phase-change random access memory (PRAM). PRAM is one of the most promising candidates to replace Flash memory in the near future.<sup>4-9</sup>

A novel PRAM concept has been proposed by NXP.<sup>6</sup> This so-called line cell concept can be integrated into the complementary metal oxide semiconductor CMOS process flow by only a few additional lithographic steps. The active material is doped SbTe which is a fast growth material based on similar material used in high-speed and high-density storage applications such as Blu-ray rewritable disks.<sup>12-17</sup> The pure crystal growth rate (without nucleation) of this material is of interest to the research of the phase-change materials. In general, PRAM cells already have a crystalline area at the boundary of the amorphous mark from which crystallization can progress. Therefore, when PRAM cells are produced from a fast-growth material the crystallization in this material can be fast and in principle only depend on growth (not nucleation).<sup>6,18</sup>

A comparison of the data retention at elevated temperatures was made between phase-change blanket layers and PRAM line cells. Phase-change blanket films and PRAM line cells were annealed in a transmission electron microscope (TEM). During annealing a series of images was taken at constant time intervals. A procedure and

---

\* Corresponding author: B.J.Kooi@rug.nl

algorithm was developed that provides a direct measurement of the pure crystal growth rate without having problems associated with variable growth directions, variable boundary shapes or new nucleation events.

In the past we have extensively employed *in situ* heating in a TEM to determine the crystal growth rates (and to a lesser extent nucleation rates) in various types of phase-change materials.<sup>19-21</sup> The growth rates were obtained from a sequence of TEM images recorded at constant temperature as a function of crystallization time. In order to derive these growth rates, the positions of the crystallization fronts in such a sequence were determined visually. This relatively weak point of visual judgment in our previous work has been removed in our present analysis, because all analysis is automated such that it is now fully computer controlled. Therefore, the present work presents a major improvement with respect to earlier published results of the crystal growth analysis in phase change thin films.<sup>11,19-25</sup>

## 2. EXPERIMENTS

Fast-growth doped SbTe thin films with a thickness of 20 nm were deposited using DC magnetron sputtering on commercially available 25 nm thick silicon nitride TEM windows. On top of each phase-change film a 20 nm or 50 nm silicon oxide layer was deposited by RF magnetron sputtering. Such an oxide layer is essential for protective, but also allows a closer comparison with the line cells where the phase change line is surrounded by the identical oxide.

Samples were isothermally annealed at 160°C, 165°C, 170°C and 175°C by *in situ* heating in a Transmission Electron Microscope (JEOL 2010F operating at 200 kV). TEM images were taken at regular intervals after nucleation had taken place. For each temperature a complete series typically consisting of 30 images was taken. Figure 1 shows selection of images from one series.

The temperature of the TEM sample holder was accurately controlled with a Gatan model 901 SmartSet Hot Stage Controller. It employs a PID controller which allows accurate control of the temperature within  $\pm 0.5$  °C. A desired final temperature can be reached with a fast ramp rate without overshoot.

The temperature of the area that is imaged within the TEM is generally lower than the temperature of the furnace in the holder. This is because the sample consists of a very thin sheet surrounded by a vacuum. All the thermal energy has to be conducted through the sheet itself. Therefore all measurements were performed on an area as close to the edge of the silicon nitride window as possible (i.e. as close as possible to the thick Si wafer). This can be seen in Figure 1 where the silicon substrate shows up as dark corners (bottom left and right). Moreover the edge of the window could be used to correct for potential drift during heating.

In order to compare results of the blanket films with the ones holding for actual PRAM cells also relatively large cells with a length of 700 nm and a width of 300 nm were analyzed electrically in a probe station combined with a heating stage. The cells were RESET to the amorphous state (at room temperature) and then isothermally crystallized at various temperatures. During this whole process the cell resistance is monitored. Moreover, a PRAM cell in the RESET state was processed by a Focused Ion Beam system such that it could be imaged (at room temperature) and heated in the TEM in order to follow the crystallization process.

## 3. RESULTS & DISCUSSION

### 3.1 Blanket layers

An example of a few TEM images recorded during the *in situ* heating at 170 °C is shown in Figure 1. Crystals can be observed readily, because they are imaged both clearly brighter and darker than the surrounding amorphous phase. This black and white contrast of the crystals is peculiar and is caused by the transrotational nature of the crystal structure.<sup>19,26</sup> Previous crystallization studies on similar fast growth materials were performed without a capping layer.<sup>19,27</sup> During crystallization the phase-change material shrinks slightly because of the difference in density between the amorphous and the crystalline phase. The amorphous layers of the samples have a free surface where bending can occur.<sup>19</sup> The combined action of densification with movement of the crystallization front results in bending of the crystal lattice planes. These crystals tend to have a regular (often three fold symmetrical) bending shape. The amorphous phase-change layer in the present study is sandwiched between a silicon oxide and silicon

nitride layer. A free surface is therefore absent. Bending in this situation is clearly more constrained. This explains the more random black and white contrast associated with the transrotational crystal structure.

From the sequence of images it is clear that crystals nucleate at random locations and grow with more or less circular shape. The edge of the silicon nitride window appears as black triangles at the bottom left and right corners of Figure 1. This is where the thin membrane of the sample meets the thick silicon substrate. The reason to keep the edges in the images is twofold: 1. analyzing a sample area that has its temperature as close as possible to the measured temperature, 2. having a reference in the image that can be used to compensate for drift.

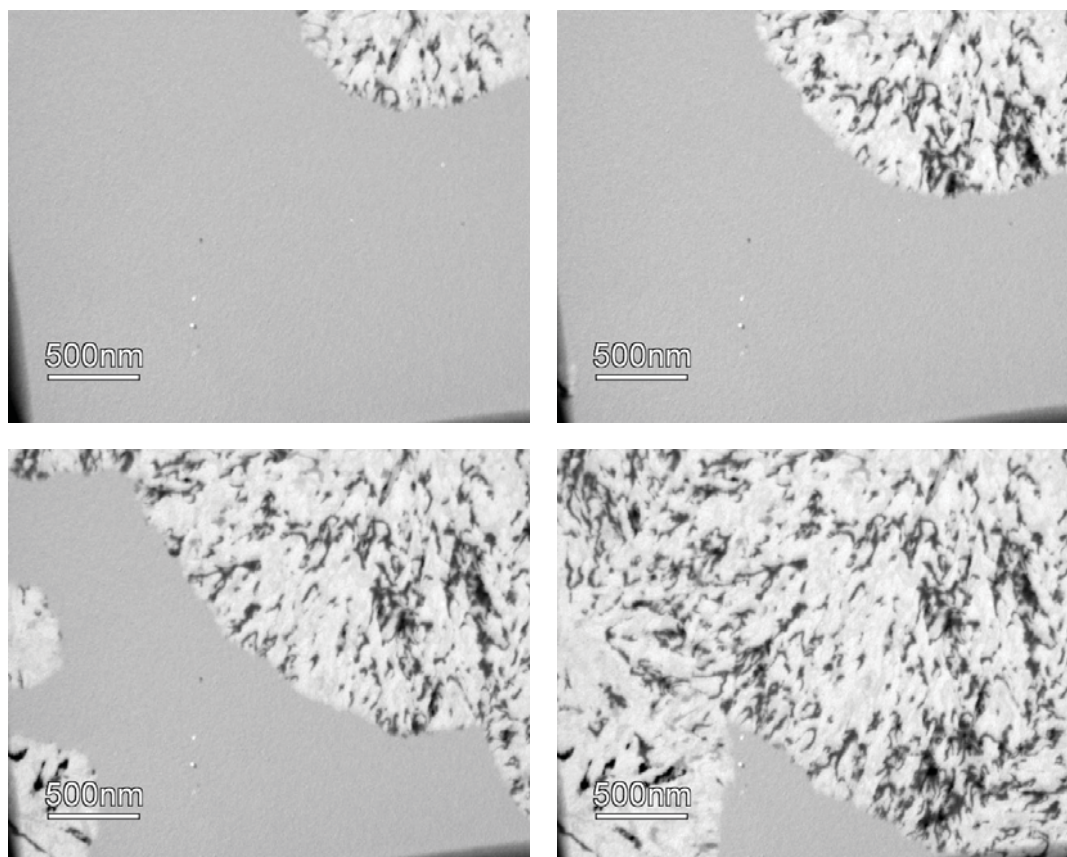


**Figure 1.** Plane view bright-field TEM images of a 20 nm thick, initially amorphous doped SbTe phase change film (between 25 nm Silicon nitride and 50 nm silicon oxide layers) taken 5, 10, 15 and 20 minutes after reaching 170 °C.

Although TEM images represent two-dimensional projections of a three-dimensional structure, the present analysis can be purely 2D, because the crystallites to be analyzed have sizes that are much larger than the 20 nm thickness of the phase-change film. In order to determine the crystal growth rate(s) at a certain temperature it is first required to quantify the position of the interface between the amorphous and crystalline phase. The procedure to do this is explained in the section 3.3.

### 3.2 PRAM line cell

A PRAM test cell of size  $700 \times 380 \text{ nm}^2$  was brought to the amorphous RESET state in a probe-station. It was prepared for TEM imaging by a focused ion beam setup (FIB). To prevent damage to the cell, a layer of several hundred nanometers of  $\text{SiO}_2$  was still surrounding the cell. This rather thick oxide layer (for TEM purposes) results in much less contrast between the crystalline and amorphous phase compared to the blanket layers. Also, electrons from the electron beam have a much higher probability to be inelastically scattered and absorbed in the oxide. Therefore, particularly at higher (annealing) temperatures, it is most likely that the electron beam damages the sample. An example of beam damage (before and after exposure) can be seen in figure 2a and b, respectively. In order to avoid

damage as much as possible, the cell was only imaged at room temperature with a relatively defocused beam (requiring long exposure times).

A TEM image of a cell before annealing is shown in Figure 2c. The cell was not fully amorphous. Figure 2d shows the same cell but after 8 subsequent anneal steps at 129°C in the TEM with the beam switched off. After 10 minutes of annealing the TEM holder was brought back to room temperature and an image was taken. The progression of the crystal front can be seen in figure 2e where each line represents the crystal boundary after an anneal step.

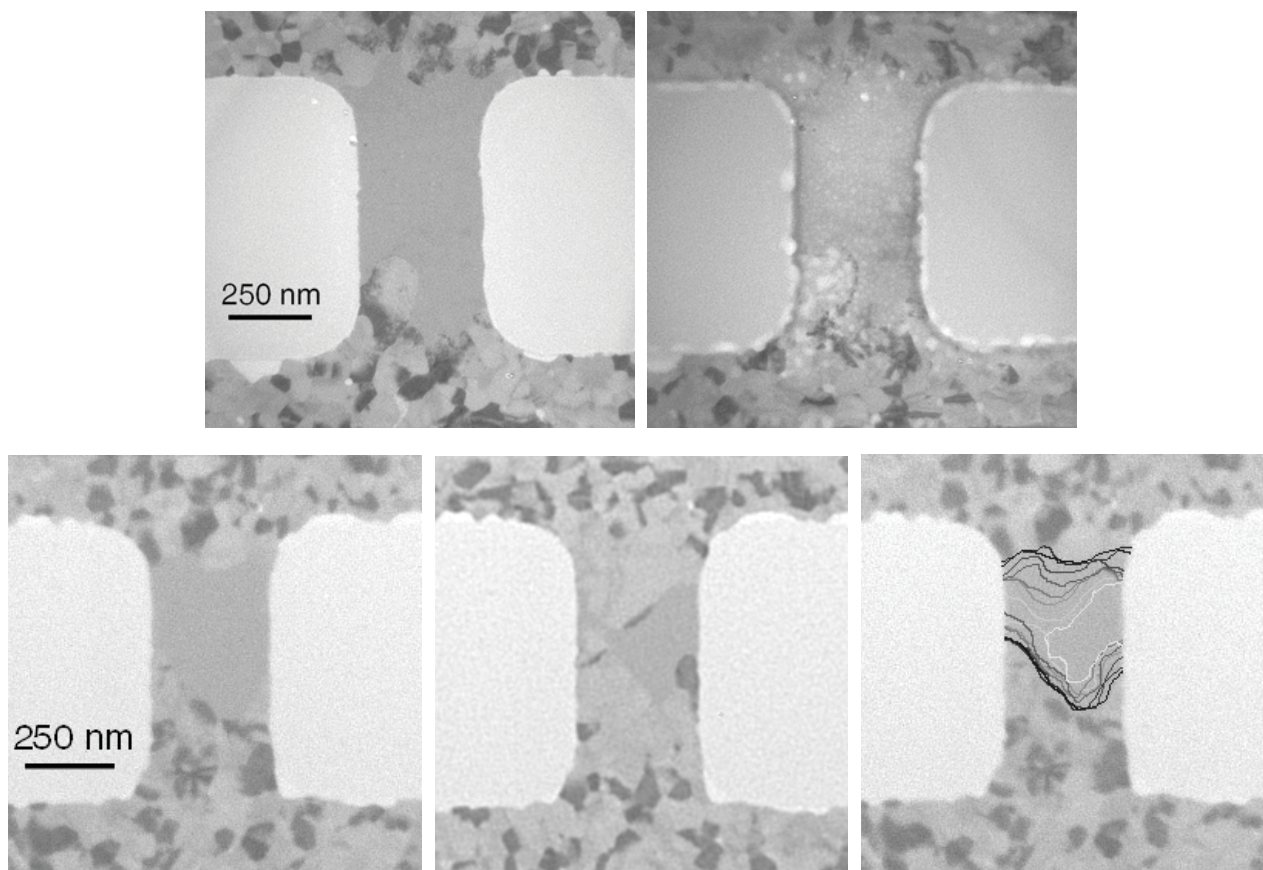


**Figure 2.** *a:* TEM image of a PRAM line cell before annealing in presence of the electron beam. *b:* Damage occurred because of the electron beam, even though the cell was not crystallized/annealed during the exposure. *c:* TEM image of a (new) PRAM line cell before annealing. Cell was not completely brought to the RESET state. *d:* image taken after eight 10 minutes anneal steps at 129 °C. Because of electron beam damage the cell could only be imaged at room temperature. *e:* The crystal fronts after each subsequent anneal step were superimposed on the image of Figure 2a.

### 3.3 Image filtering: detecting the amorphous-crystalline interface

Figure 1 illustrates that geometrical information can only be used in an early stage of crystallization. Crystals nucleate at random locations and merge with one another to form odd crystal shapes with no well defined center or radius and where after merging the crystal boundaries cannot be detected anymore. Still, the movement of the crystal boundary with time is a direct measurement of the growth rate. To quantify this movement, the location of the amorphous-crystalline interface has to be obtained from the image.

Histograms (number of pixels with a certain grey level versus the grey level) pertaining to the amorphous and crystalline phases present in an image show that the amorphous phase is represented by a bell-shaped peak, whereas the crystalline phase extends its grey levels over a much larger range including the one for the amorphous phase. The pixel values of the crystalline and the amorphous phase thus overlap. Also the image has a considerable amount of

noise. A simple threshold operation to separate the two phases does not work in this case. As a solution, a seven step filter procedure was developed by us that turns out to yield excellent results in detecting the exact position of the crystal-growth front.

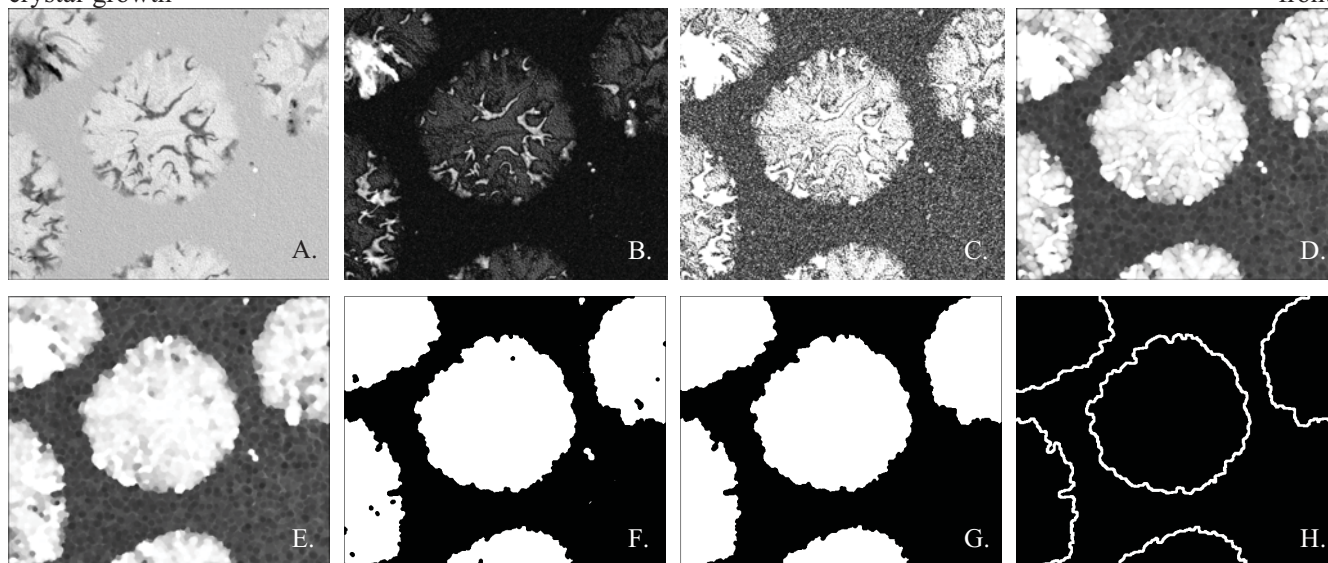


**Figure 3a:** Image before filtering. **Figure 3b – h:** Same image after filter step 1 to 7 respectively; see section 3.3 of the main text..

The seven steps followed are:

1. Subtracting the average grey level ('grey') pertaining to the amorphous phase in the series of TEM images and taking the absolute value for all pixels. This step combines the bright and dark areas pertaining to the crystalline phase and produces one uniform contrast (bright after step 1) in relation to the amorphous phase (dark after step 1); see Fig.3b.
2. Setting a maximum pixel value. Still a lot of contrast exists in the crystalline phase. Pixels above a certain value, just above the maximum value present in the amorphous phase, are given that particular value; see Fig.3c.
3. Applying an image filter that removes noise and sharpens the edges at the same time. The *mean-least-variant-filter* (MLV filter)<sup>28</sup> was used and is a crucial step in the whole procedure; see Fig.3d.
4. Performing a morphological close operation. This fuses parts of the crystalline phase not linked together (, because were related to the bright and dark parts in the original image); see Fig.3e.
5. Applying a threshold operation to create a monochrome image separating the phases. Pixel values above a certain threshold become white (crystalline), the remaining pixels are therefore automatically black and are considered amorphous; see Fig.3f.
6. Inverting small enclosed areas or spots (below a certain chosen pixel size); see Fig.3g.
7. The creation of a growth front image. This image contains a line where the white and the black areas meet after step five. This line represents the growth front; see Fig.3h.

### 3.4 Image processing: quantifying the growth speed

A complete time series of TEM images is converted into binary growth front images with the procedure delineated in section 3.3. Each growth-front image is multiplied with the value of the time (in seconds) that the image was taken. Only the growth front (line) has this time value, the rest of the image is zero. All these images in the series are summed to create a single final image that contains all essential information for determination of the crystal growth rate. In this single 'growth front - time' image each growth front is represented as a line with a pixel value equal to the time (in seconds) that the image was taken. This is shown schematically in Figure 4, where for reasons of visibility only a small selection (one out of ten) of the total number of TEM images was taken to create larger steps in time. The brighter the line the later in time the original image was taken.

At each position in the time image a statistically averaged value of the slope is found by fitting a circular surface (with a typical radius of 8 pixels) to that position and all points around it. This is graphically illustrated in Figure 4b. Only the pixels that are on a growth front are used for the fit, the black pixels (value of zero) are omitted.

Our procedure is very useful to determine the evolution of growth rate with time or crystal size (or growth-front curvature). However, our analysis shows that the crystal growth rate in our present phase-change system does not (significantly) depend on time and therefore the grey level in Figure 4c is relatively uniform (except for the boundaries where the growing crystals coalesce, because there a singularity occurs in the computer controlled determination of the growth rate).

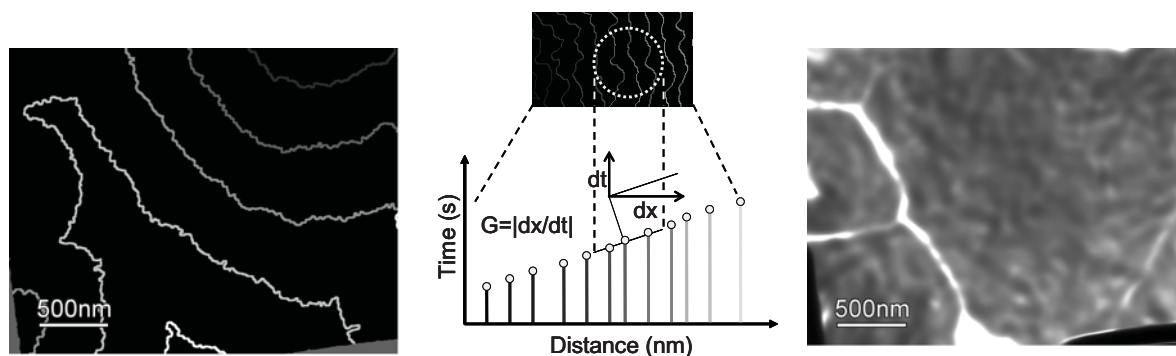


**Figure 4a:** Each line represents a crystal growth front from a series of TEM images (see Figure 1). Only one out of ten of the original images were used for this image (to create larger steps). **b:** Schematic representation of method to calculate growth rate (see section 3.4 of the main text). **c:** The (average) growth rate at each position is calculated. The location where crystals meet creates a singularity and shows as a bright line.

### 3.5. Growth rate as a function of temperature

Samples with an oxide capping layer were annealed *in situ* in the TEM at 160 °C, 165 °C, 170 °C and 175 °C. For each temperature a new sample was used. The closed data points in Figure 5 represent samples with a 50 nm silicon oxide capping layer and for the open data points the capping layer was 20 nm. After nucleation had occurred a series of images was recorded at constant time intervals until the area was crystallized. It was found that only the area that had been irradiated by the electron beam was completely crystallized. Crystals did appear in the area outside the irradiated area but these were smaller. These results indicate that the electron beam of the TEM increases the nucleation rate (decreases incubation time for nucleation) and maybe also increases the growth rate. No difference in growth was found between the samples capped with 20 nm and 50 nm silicon oxide. Assuming an Arrhenius type dependence of the growth rate on temperature an activation energy of 3.0 eV is determined by fitting the data.

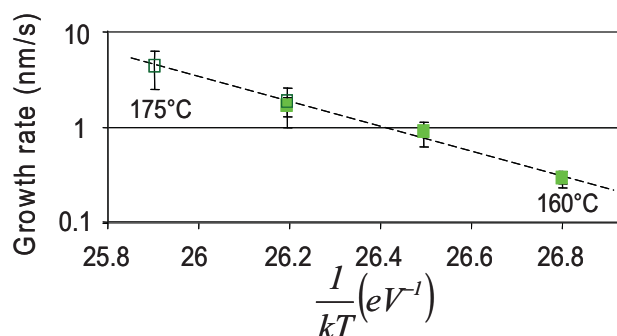


**Figure 5.** Growth rate obtained from a series of TEM images. 20 nm thick phase-change layers were sandwiched between 25 nm silicon nitride and 20 (closed squares) or 50 nm (open squares) silicon oxide.

### 3.6 Comparing retention of blanket layers with PRAM line cells

A 700x300nm<sup>2</sup> size line cell was cycled in a probe station for at least 100 RESET+SET cycles. This step avoids any starting up effects. It was RESET at room temperature and left to drift for 1000 seconds. The amorphous resistance at 1.00 second after RESET was  $3.8 \pm 0.5$  M $\Omega$  with a drift coefficient  $\alpha = 0.077 \pm 0.002$ . The cell was brought to the anneal temperature and the resistance was monitored until it crystallized (cell resistance dropped below 10 k $\Omega$ ). The actual crystallization is a very sharp transition as can be seen in Figure 6a.

The retention time is the interval between the moment the measurement temperature was reached to the crystallization event. The retention time versus the temperature is presented as an Arrhenius plot in Figure 6b. From the data the retention time at 80 °C could be extrapolated which is 10 years. An activation energy of 2.7 eV was found for growth. The retention time of the PRAM cell prepared for TEM has been added to Figure 6b (red square). The retention time was calculated from the growth rate obtained from the series of TEM images; cf. Fig.2e. Although more quantitative data is needed the value obtained is very comparable to the ones of the PRAM cell in the probe station, but deviates strongly from the ones of the blanket layers.

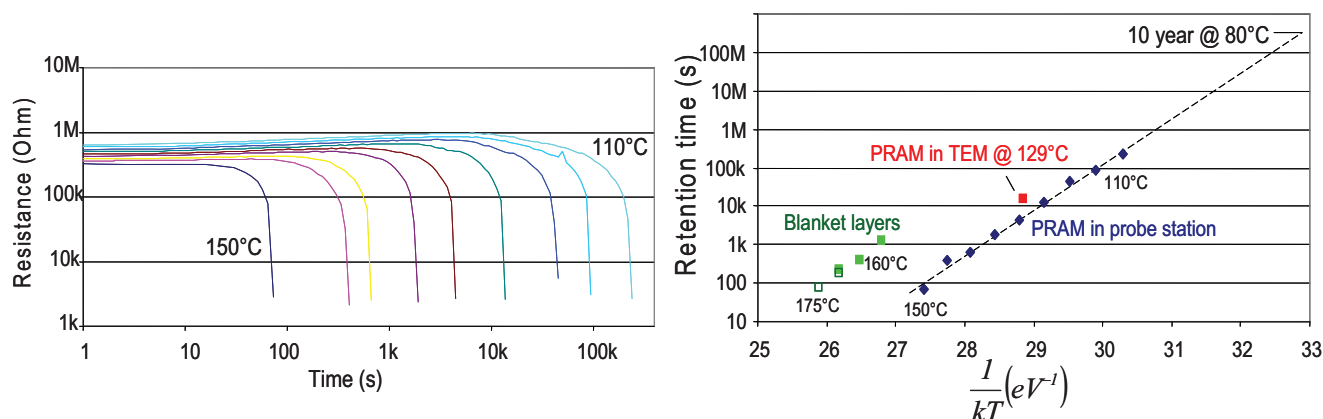


**Figure 6. a:** A  $700 \times 300 \text{ nm}^2$  PRAM line cell was brought to the amorphous state by a 50 ns RESET pulse (at room temperature). It was crystallized at a constant (high) temperature and the resistance was measured until the cell crystallized. This sequence was repeated for several temperatures in the range of 110 °C to 150 °C. **b:** Crystallization time versus the temperature is shown in an Arrhenius plot (see main text for the details of the three sample types analyzed).

From the growth rate of the blanket layers an equivalent retention time for a 700nm cell could be calculated by assuming a uniform growth of the two crystal boundaries to the center of the cell. The retention time is the time it takes for the crystal to grow half the length of the cell (from either side till they meet in the center). The result is shown Figure 6b by the green points. The activation energy of the retention time is by definition identical (apart from a minus sign) to the activation energy of growth.

Interestingly, the equivalent retention time of the blanket layers is significantly higher than the retention time of the PRAM cells (both the cell crystallized in the TEM as the cell crystallized in the probe station). A shift of about 25 °C occurs. This difference can be attributed to the fact that the PRAM cells have already been cycled, at least once as the CMOS processing crystallizes the cells. Therefore they are (always) melt-quenched by a RESET pulse. The blanket films on the other hand are as-deposited and are crystallized for the first time.

#### 4. CONCLUSIONS

Blanket doped SbTe films (20 nm thick) deposited on silicon nitride membranes and capped with 20 nm or 50 nm silicon oxide were heated at constant temperatures inside a TEM. The growth rates were obtained from a sequence of TEM images recorded at constant temperature as a function of crystallization time. The activation energy for pure growth was found to be 3.0 eV (assuming an Arrhenius type dependence of growth rate on temperature).

The retention time of a PRAM line cell was obtained in a probe station for various temperatures in the range of 110 °C to 150 °C. From the data a retention time of 10 years at 80 °C was extrapolated. Assuming an Arrhenius type dependence, an activation energy of 2.7 eV was obtained. An equivalent retention time was calculated from the growth rate of the blanket films in the TEM. This equivalent retention time was much higher than the retention time of PRAM cells measured in the probe station. This difference has to be attributed to the fact that the amorphous layer of the blanket films were as-deposited and the PRAM cell was melt-quenched (created by RESET pulse). This conclusion is corroborated by the observation that the retention time measured for a PRAM cell by in situ heating in a TEM is similar to the ones measured in a probe station.

## REFERENCES

1. M. Wuttig, N. Yamada, *Nat. Mater.* 6, 824 (2007).
2. I. Satoh, N. Yamada, *Proc. SPIE* 4085, 283 (2001).
3. J. Hellmig, A.V. Mijiritskii, H.J. Borg, K. Musialkova, and P. Vromans, *Jpn. J. Appl. Phys. Part 1*, 42, 848 (2003).
4. S. Hudgens, B. Johnson, *Mater Res. Soc. Bull.* 29, 829 (2004).
5. R. Bez, A. Pirovana, *Mater. Sci. Semicond. Proc.* 7, 349 (2004).
6. M.H.R. Lankhorst, W.S.M.M. Ketelaars, and R.A.M. Wolters, *Nat. Mater.* 4, 347 (2005).
7. W.Y. Cho et al., *IEEE J. Solid State Circuits* 40, 293 (2005).
8. A.L. Lacaíta, *Solid-State Electron.* 50, 24 (2006).
9. Y.C. Chen, C.T. Rettner, S. Raoux, G.W. Burr, S.H. Chen, R.M. Shelby, M. Salinga, W.P. Risk, T.D. Happ, G.M. McClelland, M. Breitwisch, A. Schrott, J.B. Philipp, M.H. Lee, R. Cheek, T. Nirschl, M. Lamorey, C.F. Chen, E. Joseph, S. Zaidi, B. Yee, H.L. Lung, R. Bergmann, and C. Lam, *Tech. Dig. - Int. Electron Devices Meet.* (2006).
10. G.F. Zhou, *Mater. Sci. Eng. A304-306*, 73 (2001).
11. G. Ruitenbergh, A.K. Petford-Long and R.C. Doole, *J. Appl. Phys.* 92, 3116 (2002).
12. H.J. Borg, M. van Schijndel, J.C.N. Rijpers, M.H.R. Lankhorst, G. Zhou, M.J. Dekker, I.P.D. Ubbens, and M. Kuijper, *Jpn. J. Appl. Phys. Part 1* 40, 1592 2001 .
13. N. Oomachi, S. Ashida, N. Nakamura, K. Yusu, and K. Ichihara, *Jpn. J. Appl. Phys. Part 1* 41, 1695 2002 .
14. P.K. Khulbe, T. Hurst, M. Horie, and M. Mansuripur, *Appl. Opt.* 41, 6220 2002 .
15. Y.-C. Her and Y.-S. Hsu, *Jpn. J. Appl. Phys., Part 1* 42, 804 2003.
16. M.H.R. Lankhorst, L. van Pieterse, M. van Schijndel, B.A.J. Jacobs, and J.C.N. Rijpers, *Jpn. J. Appl. Phys., Part 1* 42, 863 2003 .
17. Y.-C. Her, H. Chen, and Y.-S. Hsu, *J. Appl. Phys.* 93, 10097 2003.
18. E.R. Meinders, M.H.R. Lankhorst, *Jpn J. Appl. Phys. I* 42, 809–812 (2003).
19. B.J. Kooi and J.Th.M. De Hosson, *J. Appl. Phys.* 95, 4714 (2004).
20. B.J. Kooi, R. Pandian, J.Th.M. De Hosson and A. Pauza, *J. Mater. Res.* 20, 1825 (2005).
21. R. Pandian, B.J. Kooi, J.Th.M. De Hosson and A. Pauza, *J. Appl. Phys.* 100, 123511 (2006).
22. A.K. Petford-Long, R.C. Doole, C.N. Alfonso, and J. Solis, *J. Appl. Phys.* 77, 607 (1995).
23. M.C. Morilla, C.N. Afonso, A.K. Petford-Long, R.C. Doole, *Phil. Mag.* A73, 1237 (1996).
24. S. Privitera et al. *Mat. Res. Soc. Symp. Proc.* 803, HH1.4 (2004).
25. J. Kalb, F. Spaepen, M. Wuttig, *Appl. Phys. Lett.* 84, 5240 (2004).
26. V. Yu. Kolosov and A.R. Thölen, *Acta Mater.* 48, 1829-1840, (2000).
27. B.J. Kooi, W.M.G. Groot and J.Th.M. De Hosson, *J. Appl. Phys.* 95, 924 (2004).
28. M.A. Schulze, J.A. Pearce, *Proc. SPIE* 1902, 106 (1993).

## Biography

I am currently performing a PhD research project at the University of Groningen (The Netherlands) called “Structural and electrical switching dynamics of phase change random access memory”. The project is funded by the Materials innovation institute (M2i) and NXP semiconductors.

Still, fundamental questions have to be answered before a technological breakthrough of PRAM can be achieved. The goal of the project is to build an electrical setup and a *transmission electron microscope* (TEM) sample holder that allows for in situ switching of PRAM cells. By switching and observing single PRAM cells in the TEM valuable information about data retention and cell cycling can be obtained.